Contribution from the Institut für Physikalische und Theoretische Chemie and Physikalisches Institut, Abt. II, University of Erlangen-Nürnberg, D-8520 Erlangen, West Germany

# Mössbauer Effect and X-ray Diffraction at the High-Spin ($^5T_2$) ⇌ Low-Spin ($^1A_1$) Transition in Bis(thiocyanato)bis(4,7-dimethyl-1,10-phenanthroline)iron(II)–α-Picoline: Thermal Hysteresis, Associated Crystallographic Phase Change, Time Dependence of $^5T_2 \rightarrow {}^1A_1$ Transformation, Particle Size Effects, and Related Phenomena

E. KÖNIG,*[1a] G. RITTER,[1b] S. K. KULSHRESHTHA,[1a,c] and N. CSATARY[1b]

*Received July 27, 1983*

The iron(II) complex [Fe(4,7-$(CH_3)_2$phen)$_2$(NCS)$_2$]·α-pic (phen = 1,10-phenanthroline; α-pic = α-picoline) is shown to exhibit a high-spin ($^5T_2$) ⇌ low-spin ($^1A_1$) transition in the solid state. The ground states involved are characterized, at the transition temperature $T_c^{\uparrow}$, by $\Delta E_Q(^5T_2)$ = 2.93 mm s$^{-1}$, $\delta^{IS}(^5T_2)$ = +1.03 mm s$^{-1}$ and $\Delta E_Q(^1A_1)$ = 0.39 mm s$^{-1}$, $\delta^{IS}(^1A_1)$ = +0.40 mm s$^{-1}$. For a powdered sample, a hysteresis of $\Delta T_c$ = 56 K has been observed, the transition being centered at $T_c^{\uparrow}$ = 202 K for rising and $T_c^{\downarrow}$ = 146 K for lowering temperature. The Debye–Waller factors $-\ln f^{5}_{T_2}$ and $-\ln f_{^1A_1}$ show a different temperature dependence ($\Theta_{^5T_2} \simeq 135$ K, $\Theta_{^1A_1} \simeq 174$ K). A crystalline sample of the compound produced closely similar results with $T_c^{\uparrow}$ = 195 K and $T_c^{\downarrow}$ = 153 K ($\Delta T_c$ = 42 K). The spin transition is associated with a crystallographic phase change and is thermodynamically of first order. The temperature dependence of $n_{^5T_2}$ derived from Mössbauer-effect and X-ray diffraction data is in qualitative agreement. For decreasing temperatures below 160 K, the crystalline substance shows a significant time dependence of the $^5T_2 \rightarrow {}^1A_1$ transformation. The mean lifetime of the $^5T_2$ state, $\tau_{^5T_2}$, and the equilibrium fraction $n_{^5T_2}$ decrease as the temperature of observation decreases. The specific results depend on the crystallinity of the sample. On thorough grinding of the crystalline substance, the transition becomes very gradual with reduction of the hysteresis and a drastic increase of the residual fractions of both $^5T_2$ and $^1A_1$ states. Differences in $n_{^5T_2}$ and slight variations in $\Delta E_Q$ and $\delta^{IS}$ values as a function of temperature that have been found on repeating the measurements are believed to arise due to mobility of the crystal solvent α-picoline in the lattice.

## Introduction

Spin-crossover transitions in various iron(II) and iron(III) complexes have recently been the subject of numerous investigations.[2-4] In solution, a dynamic equilibrium between the two spin states is usually established. This is demonstrated by the approximately linear relationship between log $K$ and $1/T$, where $K = k_1/k_{-1}$ is the equilibrium constant, and by the interconversion rate constants $k_1$ and $k_{-1}$ as determined on the basis of relaxation measurements.[5,6] In solid complexes, coupling of the molecules by the lattice vibrations introduces various complications. Thus, in iron(II) spin-crossover complexes, the high-spin ($^5T_2$) ⇌ low-spin ($^1A_1$) transition is often associated with a phase change of first order. The first-order character of the transition has been established by heat capacity measurements,[7,8] the study of X-ray diffraction peak profiles,[9-11] the observation of hysteresis effects,[8-13] and the results of additional physical measurements. One of the best studied phase transitions of this type is that of the compound [Fe(4,7-$(CH_3)_2$phen)$_2$(NCS)$_2$], where 4,7-$(CH_3)_2$phen = 4,7-dimethyl-1,10-phenanthroline.[14] Investigations of the $^{57}$Fe Mössbauer effect have demonstrated[15] that the transition temperatures for rising and for lowering of temperature are $T_c^{\uparrow}$ = 121.7 K and $T_c^{\downarrow}$ = 118.6 K, respectively, the transition thus being associated with a hysteresis of the width $\Delta T_c$ = 3.1 K. A similar hysteresis is found if the X-ray diffraction of the compound is followed,[11] whereby $T_c^{\uparrow}$ = 122.9 K, $T_c^{\downarrow}$ = 119.6 K, and $\Delta T_c$ = 3.3 K are obtained. In this study, the high-spin fraction $n_{^5T_2}$ has been approximated by the intensities of X-ray diffraction peak profiles according to $n_{^5T_2} \simeq I_{^5T_2}/(I_{^5T_2} + I_{^1A_1})$.[9,11] The consistent results of these measurements provide clear evidence for a simultaneous change of metal ion spin state and crystal lattice characteristics.

For the α-picoline (α-pic) solvate of the compound, viz. [Fe(4,7-$(CH_3)_2$phen)$_2$(NCS)$_2$]·α-pic, only preliminary results of measurements of the magnetic susceptibility and the $^{57}$Fe Mössbauer effect at 298 and 77 K have been reported.[16] These data indicate an abrupt spin transition that, for decreasing temperatures, is centered at ~142 K. The result follows from the observed magnetism, since the effective magnetic moment has been found to drop suddenly from $\mu_{eff}$ = 5.05 $\mu_B$ at 144.9 K to a value of $\mu_{eff}$ = 2.69 $\mu_B$ at 141.7 K and to decrease subsequently to $\mu_{eff}$ = 1.58 $\mu_B$ at 132.1 K. The Mössbauer-effect parameters, viz. $\Delta E_Q(^5T_2)$ = 2.59 mm s$^{-1}$, $\delta^{IS}(^5T_2)$ = +0.97 mm s$^{-1}$ at 298 K and $\Delta E_Q(^1A_1)$ = 0.37 mm s$^{-1}$, $\delta^{IS}(^1A_1)$ = +0.33 mm s$^{-1}$ at 77 K, are not much different from those of the unsolvated complex, and these results indicate that the assignment of the spin transition is essentially correct. It has also been found that, for increasing temperature, the transition is taking place at a considerably higher temperature, i.e. ~200 K, although this observation has been attributed to effects related to the sample history rather than the existence of hysteresis effects.

The present study has been undertaken in order to investigate the transition in [Fe(4,7-$(CH_3)_2$phen)$_2$(NCS)$_2$]·α-pic in greater detail and, in particular, to demonstrate whether

(1) (a) Institut für Physikalische und Theoretische Chemie. (b) Physikalisches Institut, Abt. II. (c) On leave of absence from and present address at Bhabha Atomic Research Centre, Bombay 400 085, India.
(2) Goodwin, H. A. *Coord. Chem. Rev.* **1976**, *18*, 293.
(3) Martin, R. L.; White, A. H. *Transition Met. Chem.* **1968**, *4*, 113.
(4) Gütlich, P. *Struct. Bonding (Berlin)* **1981**, *44*, 83.
(5) Beattie, J. K.; Binstead, R. A.; West, R. J. *J. Am. Chem. Soc.* **1978**, *100*, 3044.
(6) Binstead, R. A.; Beattie, J. K.; Dose, E. V.; Tweedle, M. F.; Wilson, L. J. *J. Am. Chem. Soc.* **1978**, *100*, 5609.
(7) Sorai, M.; Seki, S. *J. Phys. Chem. Solids* **1974**, *35*, 555.
(8) König, E.; Ritter, G.; Kulshreshtha, S. K.; Waigel, J.; Goodwin, H. A. *Inorg. Chem.*, accompanying paper in this issue.
(9) König, E.; Ritter, G.; Irler, W.; Goodwin, H. A. *J. Am. Chem. Soc.* **1980**, *102*, 4681.
(10) König, E.; Ritter, G.; Irler, W.; Nelson, S. M. *Inorg. Chim. Acta* **1979**, *37*, 169.
(11) König, E.; Ritter, G.; Irler, W. *Chem. Phys. Lett.* **1979**, *66*, 336.
(12) Sorai, M.; Ensling, J.; Hasselbach, K. M.; Gütlich, P. *Chem. Phys.* **1977**, *20*, 197.
(13) König, E.; Ritter, G.; Kulshreshtha, S. K.; Nelson, S. M. *Inorg. Chem.* **1982**, *21*, 3022.
(14) König, E.; Ritter, G.; Kanellakopulos, B. *J. Phys. C* **1974**, *7*, 2681.
(15) König, E.; Ritter, G. *Solid State Commun.* **1976**, *18*, 279.
(16) König, E.; Ritter, G.; Madeja, K.; Böhmer, W. H. *Ber. Bunsenges. Phys. Chem.* **1973**, *77*, 390.

0020-1669/84/1323-1903$01.50/0 

hysteresis effects are of any importance. In addition, it was expected that the results might throw some light on the little-investigated effect of crystal solvent molecules on the observed high-spin ($^5T_2$) ⇌ low-spin ($^1A_1$) transition.

## Experimental Section

**Materials.** Samples of the solvated complex [Fe(4,7-$(CH_3)_2$phen)$_2$(NCS)$_2$]·α-pic were prepared by following the procedure published previously.[16] The samples gave satisfactory analyses for C, H, N, and Fe and showed very good crystallinity. A portion of the substance was mildly powdered and, for the Mössbauer studies, pressed into a Perspex sample holder (absorber I). Another portion was not subject to any physical treatment, the needlelike crystals being packed as such into a sample holder (absorber II).

**Methods.** $^{57}$Fe Mössbauer-effect spectra were measured as described in detail in previous reports.[9,10,13] All velocity scales and isomer shifts are referred to the iron standard at 298 K. To convert to the sodium nitroprusside scale, add +0.257 mm s$^{-1}$. The resulting data were corrected for nonresonant background of the γ rays, the effective thickness values $t_i$ being evaluated from the individual areas $A_i(^5T_2)$ and $A_i(^1A_1)$, $i$ = 1, 2, according to[17,18]

$$A_i = S\frac{t_i}{1 + 0.25t_i} \quad (1)$$

Here, $S$ is a scaling factor that is determined from the spectra of standard materials. From the values of $t_{^5T_2}$ and $t_{^1A_1}$, the high-spin fraction $n_{^5T_2}$ has been obtained by an iterative procedure based on the high-temperature approximation of the Debye–Waller factors.[9]

Measurements of peak profiles of the X-ray powder diffraction were carried out in the mode of step scanning of the diffractometer, the smallest step being 0.005° in 2θ. More details have been given elsewhere.[9,13,19] For the crystalline sample, the needlelike crystallites were spread out on the flat sample holder plate, and thus a high degree of texture resulted. One of the most intense lines was then chosen to study its peak profile, the areas being obtained by a least-squares fit to Gaussian line shape.

In the case of a perfectly random powder and for closely spaced diffraction lines, the $^5T_2$ fraction may be written as

$$n_{^5T_2} = \frac{R}{\alpha(T) + R[1 - \alpha(T)]} \quad (2)$$

where

$$R = \frac{I_{^5T_2}(T)}{[I_{^5T_2}(T) + I_{^1A_1}(T)]} \quad (3)$$

Here, $R$ is the observed intensity ratio of those lines that originate from the two spin phases at a temperature $T$. In eq 2, $\alpha(T)$ is the intensity ratio of the high-spin and low-spin lines if there were no spin transition involved. The temperature dependence of $\alpha(T)$ is caused by the difference in Debye–Waller factors of the two phases. It can be worked out from the intensity of the peaks in a region sufficiently distant from the transition temperature. If the two peaks are of equal intensity and the temperature dependence can be neglected, $\alpha(T)$ = 1 and hence $n_{^5T_2} = R$. This simplified case has been considered earlier.[9]

In order to investigate the time dependence of the transformation $^5T_2 \rightarrow {}^1A_1$, the sample was quickly cooled to the desired temperature, this time being referred to as $t$ = 0. Subsequently, the $^{57}$Fe Mössbauer-effect or the X-ray diffraction measurements were made within the time interval $\Delta t = t_2 - t_1$. The value of $\Delta t$ was chosen such as to be smaller than both $t_1$ and $t_2$, which quantities were measured from the time when the sample has attained the desired temperature. This observation was characterized with $t = t_1 + (\Delta t/2)$. At $t$ = 0, the sample has already acquired a finite fraction of the low-spin $^1A_1$ state, which cannot be measured experimentally, and this quantity was treated as a fitting parameter.

In order to investigate the effect of particle size on the spin transition, the crystalline substance was thoroughly ground in an agate mortar along with sintered-MgO powder. The spectra of the samples were recorded for both the cooling and heating cycles.

(17) Bykov, G. A.; Pham Zuy Hien. *Zh. Eksp. Teor. Fiz.* **1962**, *43*, 909.
(18) Lang, G. *Nucl. Instrum. Methods* **1963**, *24*, 425.
(19) Irler, W.; Ritter, G.; König, E.; Goodwin, H. A.; Nelson, S. M. *Solid State Commun.* **1979**, *29*, 39.

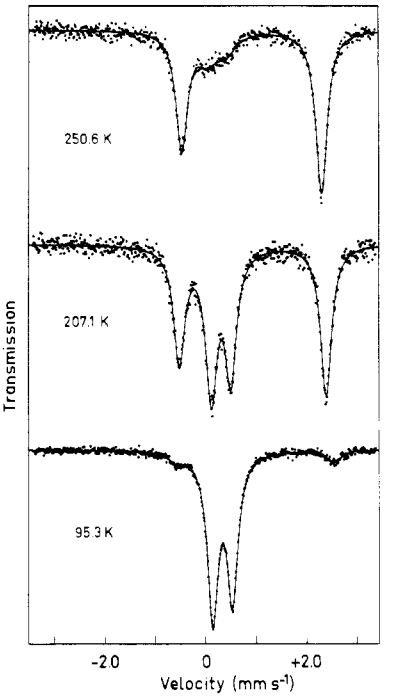


**Figure 1.** $^{57}$Fe Mössbauer-effect spectra of a powdered sample of [Fe(4,7-$(CH_3)_2$phen)$_2$(NCS)$_2$]·α-pic at 95.3, 207.1, and 250.6 K. The measurements were performed for increasing temperatures ($T_c^{\uparrow}$ = 202 K). Note that the scales for the ordinates of the individual spectra are different.

## Results

**Mössbauer-Effect Studies on a Powdered Sample.** The $^{57}$Fe Mössbauer effect for absorber I of [Fe(4,7-$(CH_3)_2$phen)$_2$(NCS)$_2$]·α-pic has been studied between 95.3 and 250.6 K. Figure 1 shows three typical spectra, i.e. at 95.3, 207.1, and 250.6 K. The dominant doublet in the spectrum at 95.3 K is characterized by the quadrupole splitting $\Delta E_Q = 0.39 \pm 0.01$ mm s$^{-1}$ and the isomer shift $\delta^{IS} = +0.44 \pm 0.01$ mm s$^{-1}$ and is thus typical for the low-spin $^1A_1$ ground state of iron(II). On the other hand, the dominant doublet in the Mössbauer spectrum at 250.6 K is typical for the high-spin $^5T_2$ ground state of iron(II), as is evident from the corresponding parameter values $\Delta E_Q = 2.78 \pm 0.01$ mm s$^{-1}$ and $\delta^{IS} = +1.01 \pm 0.01$ mm s$^{-1}$. In each of the two spectra, a small contribution of the respective other spin state is easily recognized. For increasing temperatures, the spectrum at 207.1 K contains almost equal areas of both states, the calculated value of the high-spin fraction being $n_{^5T_2} = 0.603$. The transition temperature where $n_{^5T_2} = 0.50$ then follows as $T_c^{\uparrow} = 202$ K. If the Mössbauer spectra are studied for decreasing temperatures, the transition is found to take place at a lower temperature, viz. $T_c^{\downarrow} = 146$ K. Evidently, the spin transition is associated with a hysteresis of the width $\Delta T_c = 56$ K, the hysteresis loop being illustrated in Figure 2. The detailed values of the Mössbauer parameters are listed in Table I for both increasing and decreasing temperatures.

The quadrupole doublets for both the $^1A_1$ and $^5T_2$ ground states show a significant intensity asymmetry which is due to texture effects. At 207.1 K, the intensity ratio is $I_\pi/I_\sigma = 1.31$ for the $^5T_2$ state and $I_\pi/I_\sigma = 0.87$ for the $^1A_1$ state. For both quadrupole doublets, the transitions denoted by π and σ correspond to the transitions at higher and lower energy, respectively. From Figure 2 it is evident that the transition is incomplete at both temperature ends. In addition, the hysteresis loop is asymmetric in shape, the decreasing-temperature branch being steeper than the increasing-temperature branch. The temperature dependence of the isomer shift, i.e. $\partial(\delta^{IS})/\partial T$, which is caused by the second-order Doppler effect, was found

**Table I.** $^{57}$Fe Mössbauer-Effect Parameters for a Powdered Sample of $[Fe(4,7\text{-}(CH_3)_2phen)_2(NCS)_2]\cdot\alpha$-pic[a]

| $T$, K | $\Delta E_Q(^1A_1)$,[b] mm s$^{-1}$ | $\delta^{IS}(^1A_1)$,[c] mm s$^{-1}$ | $\Delta E_Q(^5T_2)$,[b] mm s$^{-1}$ | $\delta^{IS}(^5T_2)$,[c] mm s$^{-1}$ | $n_{^5T_2}$ |
|---|---|---|---|---|---|
| | | (a) Increasing Temperatures | | | |
| 95.3 | 0.39 | +0.44 | 3.12 ± 0.02 | +1.10 ± 0.02 | 0.08 |
| 123.0 | 0.39 | +0.43 | 3.06 | +1.07 | 0.11 |
| 152.7 | 0.39 | +0.41 | 3.02 | +1.06 | 0.14 |
| 182.8 | 0.39 | +0.40 | 2.99 | +1.05 | 0.24 |
| 192.5 | 0.38 | +0.40 | 2.94 | +1.04 | 0.31 |
| 202.3 | 0.39 | +0.40 | 2.93 | +1.03 | 0.50 |
| 207.1 | 0.38 | +0.40 | 2.91 | +1.03 | 0.60 |
| 211.9 | 0.39 | +0.40 | 2.91 | +1.03 | 0.83 |
| 216.8 | 0.36 ± 0.02 | +0.34 ± 0.02 | 2.89 | +1.03 | 0.87 |
| 250.6 | 0.37 ± 0.02 | +0.31 ± 0.02 | 2.78 | +1.01 | 0.86 |
| | | (b) Decreasing Temperatures | | | |
| 206.9 | 0.38 ± 0.02 | +0.40 ± 0.02 | 2.94 | +1.04 | 0.89 |
| 201.2 | 0.38 ± 0.02 | +0.39 ± 0.02 | 2.95 | +1.05 | 0.88 |
| 192.5 | 0.41 ± 0.02 | +0.41 ± 0.02 | 2.97 | +1.05 | 0.90 |
| 187.4 | 0.38 ± 0.02 | +0.41 ± 0.02 | 2.98 | +1.05 | 0.88 |
| 179.0 | 0.36 ± 0.02 | +0.43 ± 0.02 | 2.98 | +1.06 | 0.87 |
| 157.4 | 0.40 | +0.44 | 3.02 | +1.08 | 0.83 |
| 152.7 | 0.38 | +0.44 | 3.03 | +1.08 | 0.78 |
| 149.8 | 0.38 | +0.45 | 3.03 | +1.08 | 0.69 |
| 146.8 | 0.39 | +0.45 | 3.03 | +1.09 | 0.60 |
| 143.8 | 0.38 | +0.45 | 3.04 | +1.08 | 0.42 |
| 139.9 | 0.38 | +0.45 | 3.00 | +1.08 | 0.15 |
| 133.0 | 0.38 | +0.45 | 3.02 ± 0.02 | +1.08 ± 0.02 | 0.14 |
| 113.6 | 0.38 | +0.45 | 2.98 ± 0.03 | +1.11 ± 0.02 | 0.12 |

[a] The data are listed in the order of measurement. [b] Fitting uncertainty ±0.01 mm s$^{-1}$ except where stated. [c] Isomer shifts $\delta^{IS}$ are listed relative to natural iron at 298 K; fitting uncertainty ±0.01 mm s$^{-1}$ except where stated.

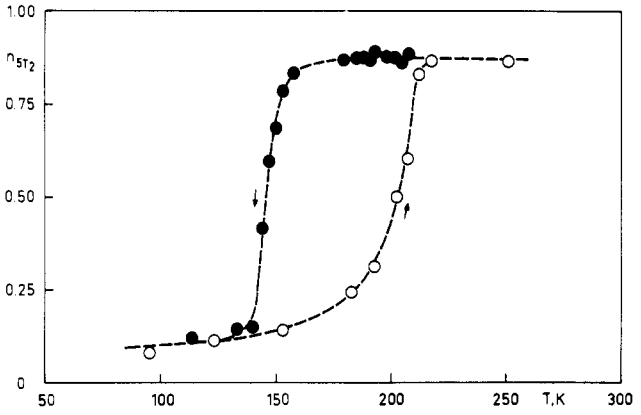


**Figure 2.** Temperature dependence of the high-spin fraction $n_{^5T_2}$ for a powdered sample of $[Fe(4,7\text{-}(CH_3)_2phen)_2(NCS)_2]\cdot\alpha$-pic (absorber I) on the basis of Mössbauer-effect measurements. A rising arrow indicates increasing temperatures, and a falling arrow indicates decreasing temperatures ($T_c^{\uparrow}$ = 202 K, $T_c^{\downarrow}$ = 146 K). Data collected with increasing temperatures are marked O; those obtained with decreasing temperatures are marked ●.

**Table II.** Debye-Waller Factors $-\ln f^{^5T_2}$ and $-\ln f^{^1A_1}$ for a Powdered Sample of $[Fe(4,7\text{-}(CH_3)_2phen)_2(NCS)_2]\cdot\alpha$-pic[a]

| $T$, K | $-\ln f^{^5T_2}$ | $-\ln f^{^1A_1}$ | $T$, K | $-\ln f^{^5T_2}$ | $-\ln f^{^1A_1}$ |
|---|---|---|---|---|---|
| | | (a) Increasing Temperatures | | | |
| 95.3 | 0.77 | 0.46 | 207.1 | 1.73 | 1.12 |
| 123.0 | 1.09 | 0.63 | 211.9 | 1.72 | 1.08 |
| 152.7 | 1.23 | 0.77 | 216.8 | 1.80 | 1.14 |
| 182.8 | 1.48 | 0.95 | 250.6 | 2.09 | 1.35 |
| 192.5 | 1.56 | 1.01 | 308.0 | 2.93 | 2.04 |
| 202.3 | 1.63 | 1.04 | | | |
| | | (b) Decreasing Temperatures | | | |
| 206.9 | 1.66 | 1.03 | 157.4 | 1.29 | 0.79 |
| 204.2 | 1.68 | 1.06 | 152.7 | 1.24 | 0.76 |
| 201.2 | 1.64 | 1.03 | 149.8 | 1.24 | 0.77 |
| 197.4 | 1.62 | 1.02 | 146.8 | 1.22 | 0.76 |
| 192.5 | 1.54 | 0.95 | 143.8 | 1.21 | 0.76 |
| 190.5 | 1.54 | 0.96 | 139.9 | 1.18 | 0.76 |
| 187.4 | 1.53 | 0.95 | 133.0 | 1.12 | 0.72 |
| 184.8 | 1.52 | 0.95 | 113.6 | 0.97 | 0.62 |
| 179.0 | 1.46 | 0.90 | | | |

[a] The data are listed in the order of measurement.

to be slightly larger for the $^5T_2$ phase than for the $^1A_1$ phase. The absorber line widths for the residual fractions were found to be larger than the values for the bulk material. The values of the Debye–Waller factors obtained on the basis of the high-temperature approximation show significant differences for the two spin phases. The detailed values are listed in Table II. The Debye temperatures derived from the temperature dependence of $-\ln f_i$ (i = $^5T_2$, $^1A_1$) with use of $M$ = 57 au are $\Theta_{^5T_2} \simeq 135$ K and $\Theta_{^1A_1} \simeq 174$ K.

**Mössbauer-Effect Studies on a Crystalline Sample.** A sample of the compound $[Fe(4,7\text{-}(CH_3)_2phen)_2(NCS)_2]\cdot\alpha$-pic consisting of needlelike crystals of length between 0.10 and 0.30 mm (absorber II) has been studied between 91.0 and 305.0 K. The $^{57}$Fe Mössbauer effect at 91.0 K showed a low-spin $^1A_1$ spectrum characterized by $\Delta E_Q$ = 0.39 ± 0.01 mm s$^{-1}$, $\delta^{IS}$ = +0.43 ± 0.02 mm s$^{-1}$, and $n_{^5T_2}$ = 0.09. At the temperature of 251.0 K, the high-spin $^5T_2$ spectrum produced $\Delta E_Q$ = 2.78 ± 0.01 mm s$^{-1}$, $\delta^{IS}$ = +1.02 ± 0.02 mm s$^{-1}$, and $n_{^5T_2}$ = 0.89. These results are practically identical with those of the powdered sample (viz. absorber I), and therefore, the data for absorber II at the intermediate temperatures are not listed in detail. Measurements for both increasing and decreasing temperatures resulted in transition temperatures $T_c^{\uparrow} \simeq 195$ K and $T_c^{\downarrow} \simeq 153$ K and a hysteresis loop of width $\Delta T_c$ = 42 K. The detailed values of $n_{^5T_2}$ are plotted, as a function of temperature, in Figure 3. It should be noted that the sample showed a significant time dependence of the $^5T_2 \rightarrow {}^1A_1$ transformation for decreasing temperatures. The values of $n_{^5T_2}$ that have been employed in Figure 3 are equilibrium values of the $^5T_2$ fraction. These values have been obtained by keeping the sample for several hours at the desired temperature before data accumulation. For comparison, the nonequilibrium values of $n_{^5T_2}$ obtained just after cooling of the sample have also been included in the figure.

The values of $T_c$ and $\Delta T_c$ are quite different for the powdered sample (absorber I) and the crystalline sample (absorber

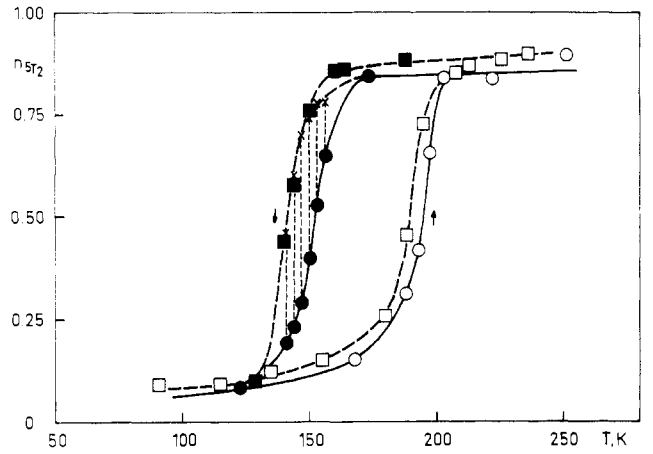


**Figure 3.** Temperature dependence of the high-spin fraction $n_{^5T_2}$ for a crystalline sample of [Fe(4,7-$(CH_3)_2$phen)$_2$(NCS)$_2$]·α-pic (absorber II)). Data collected with increasing temperatures are marked ○; those obtained with decreasing temperatures are marked ●. Broken lines on the falling branch of the hysteresis loop indicate the time dependence of $n_{^5T_2}$ for the $^5T_2 \rightarrow {}^1A_1$ transformation, the initial values being marked ×. □ and ■ correspond to the second set of measurements on the same absorber.

II) of the substance. Possible explanations might involve the effect of crystallite size or some other little controlled changes within the lattice of the substance. In order to throw some light on these aspects of our study, the measurements for absorber II were repeated after a period of several months. The results of this set of observations were again different; i.e. $T_c^{\uparrow} \simeq 189$ K and $T_c^{\downarrow} \simeq 142$ K were obtained. Both values are considerably lower than those of the previous measurements listed above (cf. Figure 3). In the course of the studies it was observed that, after each temperature cycle, the sample showed clear indication of cracking of the crystallites, which could be the reason for the changes of the $T_c$ values. In addition, the cracking suggests that the spin transition is associated with a crystallographic phase change.

**X-ray Diffraction Studies on a Crystalline Sample.** Variable-temperature X-ray diffraction patterns for the needlelike crystallites of [Fe(4,7-$(CH_3)_2$phen)$_2$(NCS)$_2$]·α-pic were recorded for $2\theta$ values from 8° onward. In general, a single intense peak along with a number of weak lines was observed for the temperature region where essentially only one of the spin states was present. The position and intensity of this characteristic line is quite different for the two spin states, $^5T_2$ and $^1A_1$. Within the temperature region where both spin states coexist, the diffraction patterns show both of these lines, the intensity of the lines varying consistently with the change of spin state as derived, e.g. from the Mössbauer-effect studies. Figure 4 illustrates position and intensity of the two diffraction lines at four selected temperatures. The derived values of the interplanar separations corresponding to these lines are, at 160 K, $d_{^1A_1} = 9.476$ Å and $d_{^5T_2} = 9.203$ Å. This finding establishes that the high-spin ($^5T_2$) ⇌ low-spin ($^1A_1$) transition in [Fe(4,7-$(CH_3)_2$phen)$_2$(NCS)$_2$]·α-pic is associated with a crystallographic phase change. The observed decrease in the value of $d_{hkl}$ for the $^5T_2$ phase should not be taken as an indication for a reduction in volume of the molecule on a $^1A_1 \rightarrow {}^5T_2$ transformation, since, for a crystallographic phase transition, the Miller indices *hkl* corresponding to the two reflections may not be the same. Also the existence of residual fractions at both high and low temperatures is clearly evident from Figure 4.

Similar to the Mössbauer-effect studies, the crystallographic phase transition shows hysteresis effects. For increasing temperatures, the transition takes place at $T_c^{\uparrow} \simeq 190$ K, whereas for decreasing temperatures, the transition is observed

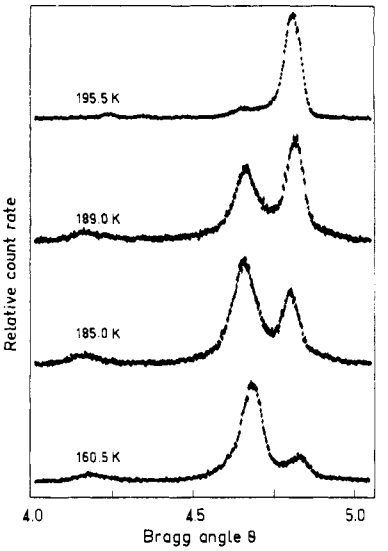


**Figure 4.** X-ray peak profiles for a crystalline sample of [Fe(4,7-$(CH_3)_2$phen)$_2$(NCS)$_2$]·α-pic at 160.5, 185, 189, and 195.5 K. The temperatures correspond to the increasing branch of the hysteresis loop. Note that the scales for the ordinates of the individual diffraction patterns are different.

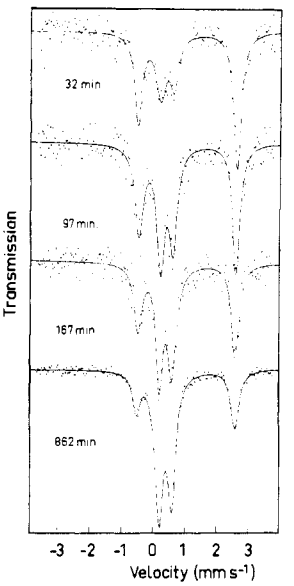


**Figure 5.** $^{57}$Fe Mössbauer-effect spectra of a crystalline sample of [Fe(4,7-$(CH_3)_2$phen)$_2$(NCS)$_2$]·α-pic recorded at $T = 147$ K as a function of time. The time interval to record the spectra is $\Delta t = 60$ min, except for the spectrum after 862 min, where $\Delta t = 600$ min.

around $T_c^{\downarrow} \simeq 155$ K. The values of the intensity ratio $R$ were found to follow a reasonably smooth curve. Nevertheless, calculated values of the high-spin fraction $n_{^5T_2}$, based on these observations, did not produce the desired consistency of results. It is believed that this arises because of the significant texture effects and the cracking of the crystallites during phase transition, which introduces considerable uncertainties into the estimation of the $\alpha(T)$ term in eq 2.

**Time Dependence of the $^5T_2 \rightarrow {}^1A_1$ Transformation.** In Figure 5, the $^{57}$Fe Mössbauer spectra recorded for different time instants at $T = 147$ K are displayed for the crystalline sample of [Fe(4,7-$(CH_3)_2$phen)$_2$(NCS)$_2$]·α-pic (absorber II). From the figure it is evident that, as the time passes on, the sample continuously changes from the high-spin $^5T_2$ to the low-spin $^1A_1$ state. Similar observations have been made for several other temperatures, i.e. $T = 156$, 153, 144, and 141 K, which all are situated on the falling branch of the hysteresis loop. The derived values of the high-spin fraction, $n_{^5T_2}$, cor-

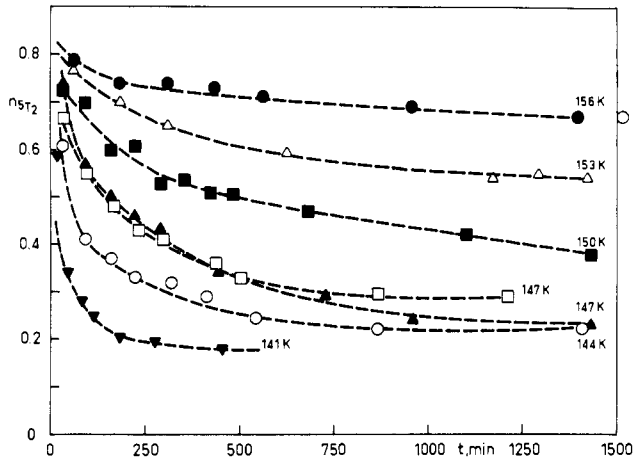


**Figure 6.** High-spin fraction $n_{^5T_2}$ for a crystalline sample of [Fe(4,7-$(CH_3)_2$phen)$_2$(NCS)$_2$]·α-pic as a function of time. The data have been obtained on the basis of Mössbauer-effect measurements. The temperatures refer to the falling branch of the hysteresis loop. Corresponding points are connected by dashed auxiliary lines.

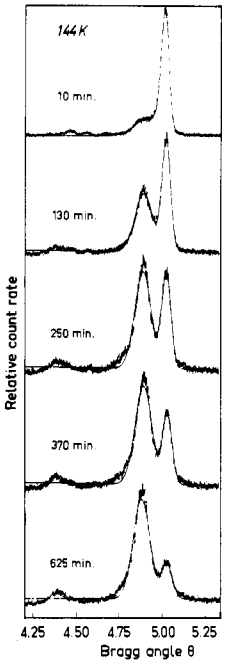


**Figure 7.** X-ray peak profiles for a crystalline sample of [Fe(4,7-$(CH_3)_2$phen)$_2$(NCS)$_2$]·α-pic at $T$ = 144 K as a function of time. The time of observation is $\Delta t$ = 10 min for each diffraction pattern. Values of $2\theta$ on the abscissa are not corrected for a misalignment of 0.4°.

responding to these temperatures are plotted in Figure 6 as a function of the time of measurement. From the figure it may be seen that, at $t$ = 0, the system has already acquired a finite fraction of the $^1A_1$ phase, $1 - n_0^{^5T_2}$, and the value of this quantity increases as the temperature of measurement is decreased. Secondly, even after a sufficiently long time period (cf. $t \approx 1500$ min), the transformation is not complete, and the limiting value of the high-spin fraction, $n_\infty^{^5T_2}$, decreases as the temperature of measurement is decreased.

In Figure 7, the time dependence of the X-ray diffraction peak profiles for the selected intense Bragg peaks is displayed at $T$ = 144 K for the crystalline sample of the substance. Here one can easily follow the progress of the crystallographic phase change that is associated with the $^5T_2 \rightarrow {}^1A_1$ transformation. The calculated values of $R = I_{^5T_2}/(I_{^5T_2} + I_{^1A_1})$, which qualitatively represent the high-spin fraction, $n_{^5T_2}$, have been plotted, in Figure 8, as a function of time for a number of additional temperatures, i.e. $T$ = 155, 150, 144, and 131 K. In a

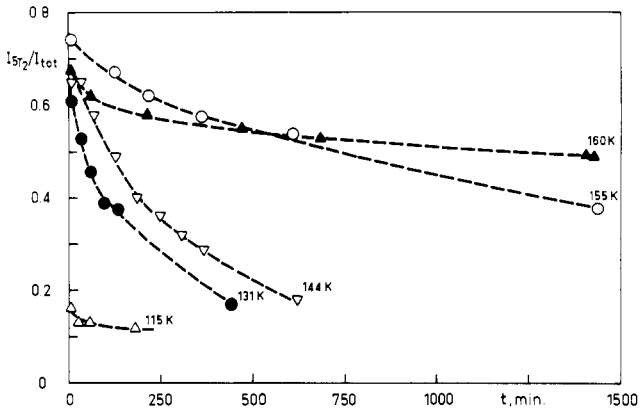


**Figure 8.** Area ratio $R = I_{^5T_2}/I_{total}$ for a crystalline sample of [Fe(4,7-$(CH_3)_2$phen)$_2$(NCS)$_2$]·α-pic as a function of time. The data have been obtained on the basis of X-ray diffraction measurements. The temperatures refer to the falling branch of the hysteresis loop. Corresponding points are connected by dashed auxiliary lines.

qualitative way, these curves are similar to those obtained on the basis of the $^{57}$Fe Mössbauer effect, viz. Figure 6, although some differences are apparent.

From both these figures it is clear that, as the temperature is decreased, the $^5T_2 \rightarrow {}^1A_1$ transformation becomes faster and the value of the residual $^5T_2$ fraction decreases.

To estimate the mean lifetime $\tau_{^5T_2}$ of the $^5T_2$ state at a particular temperature $T$, the observed values of the high-spin fraction $n_{^5T_2}$ derived from the Mössbauer spectra were fitted to the exponential function

$$n_t^{^5T_2} = n_\infty^{^5T_2} + (n_0^{^5T_2} - n_\infty^{^5T_2})e^{-t/\tau_T} \qquad (4)$$

In eq 4, $n_0^{^5T_2}$ is the value of the high-spin fraction at $t$ = 0 and $n_\infty^{^5T_2}$ is the value of the residual high-spin fraction corresponding to $t = \infty$. In the numerical procedure, the quantities $n_0^{^5T_2}$, $n_\infty^{^5T_2}$, and $\tau_T$ were treated as fitting parameters. Unfortunately, the fitting procedure did not produce the desired convergence, thus indicating that, for the present complex, the $^5T_2 \rightarrow {}^1A_1$ transformation cannot be described by a time dependence as simple as that of eq 4. The reason for this behavior will become clear below.

It may be mentioned that when the time dependence measurements were repeated at the same temperature, the consistency of the results was rather poor for both Mössbauer-effect and X-ray diffraction studies. This may be seen, in Figure 6, from the values of $n_{^5T_2}$ at $T$ = 147 K and, in Figure 8, from the values of $R$ at $T$ = 144 K.

In order to investigate the time dependence of the $^1A_1 \rightarrow {}^5T_2$ transformation, similar measurements as above were carried out for the increasing branch of the hysteresis loop with use of both Mössbauer-effect and X-ray diffraction methods. In spite of the fact that the observations were made for an extended period of time and at a number of temperatures, no detectable time dependence of the $^1A_1 \rightarrow {}^5T_2$ transformation could be observed.

**Effect of Grinding of the Crystalline Substance.** In order to improve our understanding of the effect of sample crystallinity on the spin transition, the crystals of [Fe(4,7-$(CH_3)_2$phen)$_2$(NCS)$_2$]·α-pic were ground in an agate mortar. This procedure resulted in an almost semisolid material that stuck to the surface of the mortar. To avoid this property of the material, the substance was ground with sintered magnesium oxide (absorber III). The $^{57}$Fe Mössbauer spectra of this absorber were recorded for both increasing- and decreasing-temperature cycles. The results showed a drastic change in the temperature dependence of $n_{^5T_2}$, as seen in Figure 9c, where the values of $t_{^5T_2}/t_{total}$ are plotted. It should be noted that these values would represent the high-spin fraction $n_{^5T_2}$

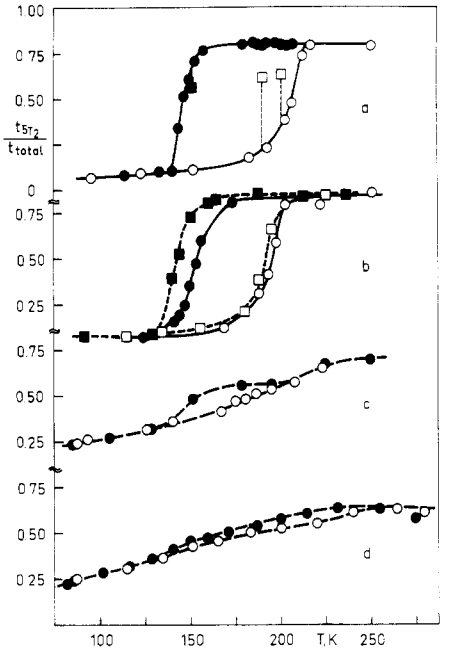


**Figure 9.** Temperature dependence of the relative effective thickness $t_{^5T_2}/t_{total}$ for $[Fe(4,7\text{-}(CH_3)_2phen)_2(NCS)_2]\cdot\alpha$-pic. Data collected with increasing temperatures are marked with open symbols, and those obtained with decreasing temperatures are marked with solid symbols: (a) mildly powdered sample (absorber I; squares refer to measurements repeated after 2 years); (b) crystalline sample (absorber II; two sets of measurements recorded within the period of about 6 months are shown by circles and squares, respectively; (c) substance ground with sintered-MgO powder (absorber III); (d) same sample as (c), measurement repeated after a period of 2 months.

if the Debye–Waller factors for the two phases, $^5T_2$ and $^1A_1$, were equal. Evidently, the transition assumes a practically continuous appearance and is spread out over the entire temperature range between 80 and 280 K. The values of the residual fractions at the temperature ends change drastically, and the thermal hysteresis loop becomes rather narrow. Moreover, the texture-based intensity asymmetry of the quadrupole doublets has changed, typical values at 207.3 K being $I_\pi/I_\sigma = 0.925$ for the $^5T_2$ and $I_\pi/I_\sigma = 0.974$ for the $^1A_1$ state. After approximately 2 months, a certain difference in the values of $t_{^5T_2}/t_{total}$ was encountered, although the general behavior of the results was similar (cf. Figure 9d). This absorber was also measured at 4.2 K to determine the residual $^5T_2$ fraction, the result of $t_{^5T_2}/t_{total} = 0.25$ being almost equal to the value at 85 K. Also the temperature at which $n_{^5T_2} = 0.50$ is significantly different for the ground sample as compared to that for the absorbers I and II. The result is obtained partly because of the increase in the residual $^5T_2$ fraction. Prompted by these results, we finally remeasured the original absorber I at a number of selected temperatures, after it had been stored for about 2 years. The resulting values of $t_{^5T_2}/t_{total}$ were found to be again different from those obtained earlier.

All these observations show the important effect of the crystalline state and the history of the specimen on the spin transition. Possible explanations for some of the observations will be discussed below.

**Quadrupole Splitting and Isomer Shift for Different Samples.** In Figure 10, the quadrupole splitting $\Delta E_Q$ and the isomer shift $\delta^{IS}$ for the high-spin $^5T_2$ phase are presented as a function of temperature. The data for three different absorbers, viz. absorbers I, II, and III, are displayed, including two sets referring to absorber III. Evidently, there is a significant distribution of the values of $\Delta E_Q(^5T_2)$ for the different samples, whereas consistency of the results is preserved for each individual set of measurements. The variation of the values at

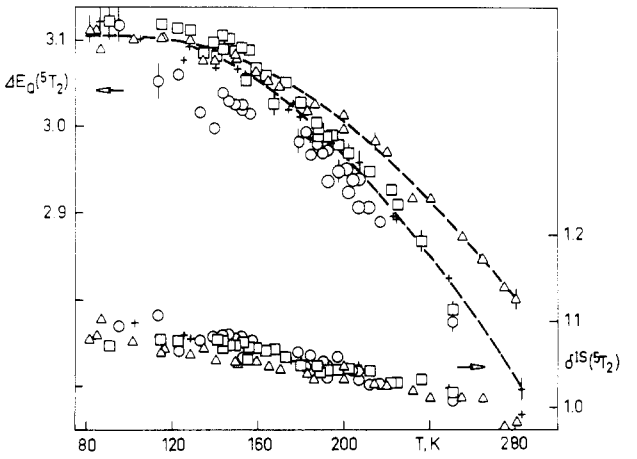


**Figure 10.** Temperature dependence of the quadrupole splitting $\Delta E_Q(^5T_2)$ and the isomer shift $\delta^{IS}(^5T_2)$ for different samples of $[Fe(4,7\text{-}(CH_3)_2phen)_2(NCS)_2]\cdot\alpha$-pic: (○) powdered sample (absorber I); (□) crystalline sample (absorber II); (+) substance ground with sintered MgO (absorber III), first measurement; (△) same absorber after a period of 2 months. The two sets of measurements for absorber III are connected by dashed lines.

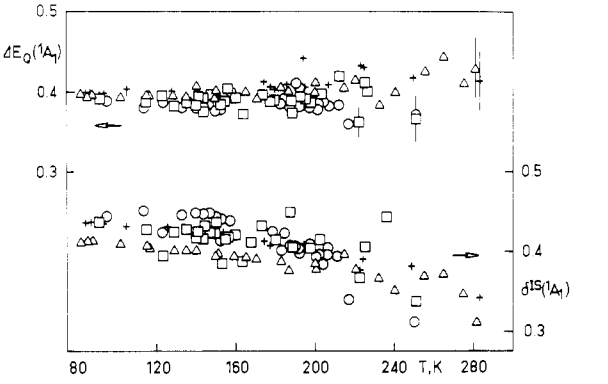


**Figure 11.** Temperature dependence of the quadrupole splitting $\Delta E_Q(^1A_1)$ and the isomer shift $\delta^{IS}(^1A_1)$ for different samples of $[Fe(4,7\text{-}(CH_3)_2phen)_2(NCS)_2]\cdot\alpha$-pic: (○) powdered sample (absorber I); (□) crystalline sample (absorber II); (+) substance ground with sintered MgO (absorber III), first measurement; (△) same absorber after a period of 2 months.

any one temperature is seen to be larger than the estimated margin of error for that quantity. The corresponding errors have been marked, in Figure 10, for a selected number of data points. The temperature dependence of $\Delta E_Q(^5T_2)$, which is characterized by a dashed line, is as expected for a $^5T_2$ ground state of iron(II). Moreover, the isomer shift $\delta^{IS}(^5T_2)$ also shows a distribution of values that is larger than the average margin of error. Note that the latter is smaller than the error associated with $\Delta E_Q(^5T_2)$. Also, the distribution becomes wider as the temperature of measurement is being increased. In Figure 11, the values of $\Delta E_Q$ and $\delta^{IS}$ for the low-spin $^1A_1$ phase are displayed in order to demonstrate the distribution of these values for the different sets of measurements. At the lower temperatures, the values of $\Delta E_Q(^1A_1)$ seem to converge, whereas beyond $T_c$, the variation of the values becomes considerably larger. Similarly, the distribution of the values of $\delta^{IS}(^1A_1)$ is outside the estimated margin of error, in particular at the lower temperatures, where this error is quite small.

## Discussion

The results reported above show clearly that the compound $[Fe(4,7\text{-}(CH_3)_2phen)_2(NCS)_2]\cdot\alpha$-pic is involved in a high-spin ($^5T_2$) $\rightleftharpoons$ low-spin ($^1A_1$) transition within the temperature range studied. There are several pieces of evidence which indicate that the transition is associated with a phase change of first

order. Thus it has been demonstrated that, for the powdered sample, the Debye temperatures $\Theta_{^5T_2}$ and $\Theta_{^1A_1}$ are significantly different. This fact implies different phonon spectra for the two phases and consequently a crystallographic rearrangement of the lattice. The conclusion is supported by the difference in the values of $\partial(\delta^{IS})/\partial T$ for the two phases, $^5T_2$ and $^1A_1$, since, in the harmonic approximation, these quantities and the corresponding Debye–Waller factors are directly related.[20]

An additional characteristic property of phase transitions of first order is the observation of hysteresis effects, and indeed, a hysteresis of width $\Delta T_c$ = 56 K has been found for the powdered sample of the compound (absorber I). For the crystalline sample studied by $^{57}$Fe Mössbauer effect (absorber II), a similar hysteresis of width $\Delta T_c$ = 42 K has been observed. Thus far, an *abrupt* high-spin ($^5T_2$) ⇌ low-spin ($^1A_1$) transition associated with hysteresis effects has been reported for a number of iron(II) compounds. These systems include[21] $[Fe(phy)_2](BF_4)_2$[8] and $[Fe(phy)_2](ClO_4)_2$,[9] $[Fe(bt)_2(NCS)_2]$,[10] $[Fe(paptH)_2](NO_3)_2$,[22] $[Fe(2\text{-}pic)_3]Cl_2\cdot H_2O$,[12] $[Fe(bi)_3](ClO_4)_2$,[13] and $[Fe(4,7\text{-}(CH_3)_2phen)_2(NCS)_2]$.[11,15] Very recently, the observation of a hysteresis of width $\Delta T_c \simeq 0.15$ K has been claimed[23] for the *extracted* sample of the classical spin transition complex $[Fe(phen)_2(NCS)_2]$.[24] However, there are various controversial results[25,26] for the pure precipitated and the metal-diluted $[Fe(phen)_2(NCS)_2]$, the significance of which is not clear.

Additional evidence for the first-order character of the transition, or at least for an associated crystallographic phase change, is provided by the changes observed in the X-ray diffraction studies. These measurements have been performed in detail for the crystalline sample, and a hysteresis curve similar to that generated on the basis of the $^{57}$Fe Mössbauer effect was obtained. In complete analogy to previous studies,[8-11] the results show that the transformation of metal ion spin state and the change of crystal lattice are simultaneous processes. It should be noted that, in contrast to the observations reported here, no separate X-ray diffraction lines have been found for compounds that exhibit a *continuous* type high-spin ($^5T_2$) ⇌ low-spin ($^1A_1$) transition. Examples for this type of behavior are found in[27] $[Fe(bts)_2(NCS)_2]$,[28] $[Fe(4\text{-}paptH)_2]X_2\cdot 2H_2O$ (X = $ClO_4$, $BF_4$),[29] and $[Fe(dppen)_2Cl_2]\cdot 2(CH_3)_2CO$.[30] In these systems, the Bragg reflections show only a systematic shift in their positions due to the volume change associated with the spin transition, since a crystallographic phase transformation is not involved.

In order to comment on the effect of solvation, a comparison of the present results with those of the unsolvated complex, $[Fe(4,7\text{-}(CH_3)_2phen)_2(NCS)_2]$, may be of interest. In the unsolvated complex, the spin transition is centered at $T_c^{\uparrow}$ = 121.7 K for rising and at $T_c^{\downarrow}$ = 118.6 K for lowering temperature, the width of the resulting hysteresis loop being $\Delta T_c$ = 3.1 K.[11,15] The corresponding values for the powdered sample of the $\alpha$-picoline solvate are $T_c^{\uparrow}$ = 202 K, $T_c^{\downarrow}$ = 146 K, and thus $\Delta T_c$ = 56 K. The values of the quadrupole splitting $\Delta E_Q(^5T_2)$ are almost equal for the unsolvated and the solvated complexes, their temperature dependences being identical. On the other hand, the values of $\Delta E_Q(^1A_1)$ are slightly larger for the unsolvated than for the solvated complex, typical values being $\Delta E_Q(^1A_1) \simeq 0.47$ and 0.39 mm s$^{-1}$, respectively, almost independent of temperature. The isomer shifts for the two complexes are identical within the experimental uncertainty. Thus, whereas the usual Mössbauer parameters like $\Delta E_Q$ and $\delta^{IS}$ are little affected, the transition temperatures $T_c^{\uparrow}$ and $T_c^{\downarrow}$ are considerably different, the hysteresis curve being of much smaller width and being considerably sharper for the unsolvated than for the solvated complex. Evidently, only the characteristic properties of the solid are affected by solvation, the electron distribution at the iron(II) ion remaining essentially unchanged. In some of our recent studies,[8-10] we have shown that spin transitions may proceed via the formation of domains of the minority spin molecules, i.e. of both $^5T_2$ and $^1A_1$ states in the respective regions of temperature. It is expected that the initial formation as well as the growth of the domains will be dependent on the defect structure of the solid. Such defects will involve vacancies, dislocations, grain boundaries, and other local nonuniformities.[31] Solvates may show additional defects which could result from disorder or from the loss of a small number of solvent molecules. This could explain why, in the $\alpha$-picoline solvate of $[Fe(4,7\text{-}(CH_3)_2phen)_2(NCS)_2]$, the spin transition is less abrupt and the hysteresis loop is of considerably larger width than in the unsolvated complex. On the other hand, the observed gross changes in the spin transition characteristics for different absorbers of the present complex are certainly not due to any measurable loss of the crystal solvent from the lattice, since, in that case, there should be a discontinuity in $n_{^5T_2}$ around 120 K, i.e. around $T_c$ for unsolvated $[Fe(4,7\text{-}(CH_3)_2phen)_2(NCS)_2]$, and there should also be no significant $n_{^5T_2}$ values below that temperature.

In the following, we assume that the $\alpha$-picoline molecules are not very strongly bound in the crystal lattice and that these possess a certain mobility at room temperature. If this assumption is correct, the solvent will be quickly frozen in positions that are not the equilibrium positions if the sample is quenched from room to lower temperatures. It will then take a finite time to relax from this state to the equilibrium state, thus producing the observed time dependence of the $^5T_2 \rightarrow {}^1A_1$ transformation. On the other hand, in order to study the time dependence of the $^1A_1 \rightarrow {}^5T_2$ transformation on the increasing branch of the hysteresis loop, the sample has to be quickly heated to the desired temperature from temperatures far below $T_c^{\uparrow}$. The sudden heating will result in enhanced thermal mobility of the $\alpha$-picoline molecules, and these will assume the equilibrium position in a very short time. The thermal relaxation rates for the temperatures corresponding to the increasing and the decreasing branches are significantly different because of the large width of the hysteresis loop (cf. Figure 3). This fact explains why no time dependence for the $^1A_1 \rightarrow {}^5T_2$ transformation was detected. There will be a finite time dependence of the $^1A_1 \rightarrow {}^5T_2$ transformation, even on the increasing-temperature branch, but it may be shorter than the time required to collect an acceptable Mössbauer spectrum of X-ray diffraction pattern. Moreover, the quenched positions of the $\alpha$-picoline molecules and their thermal relaxation will be dependent on the rate of quenching and on the temperature to which the sample has been quenched. This is the most

(20) Taylor, R. D.; Craig, P. P. *Phys. Rev.* **1968**, *175*, 782.
(21) The following ligand abbreviations have been used: phy = 1,10-phenanthroline-2-carbaldehyde phenylhydrazone, bt = 2,2′-bi-2-thiazoline, paptH = 2-(2-pyridylamino)-4-(2-pyridyl)thiazole, 2-pic = 2-picolylamine, bi = 2,2′-bi-2-imidazole, phen = 1,10-phenanthroline.
(22) Ritter, G.; König, E.; Irler, W.; Goodwin, H. A. *Inorg. Chem.* **1978**, *17*, 224.
(23) Müller, E. W.; Spiering, H.; Gütlich, P. *Chem. Phys. Lett.* **1982**, *93*, 567.
(24) König, E.; Madeja, K. *Inorg. Chem.* **1967**, *6*, 48.
(25) Rao, P. S.; Reuveni, A.; McGarvey, B. R.; Ganguli, P.; Gütlich, P. *Inorg. Chem.* **1981**, *20*, 204.
(26) Ganguli, P.; Gütlich, P.; Müller, E. W.; Irler, W. *J. Chem. Soc., Dalton Trans.* **1981**, 441.
(27) The following ligand abbreviations have been used: bts = 2,2′-bi(5-methyl-2-thiazoline), 4-paptH = 2-((4-methyl-2-pyridyl)amino)-4-(2-pyridyl)thiazole, dppen = *cis*-1,2-bis(diphenylphosphino)ethylene.
(28) König, E.; Ritter, G.; Kulshreshtha, S. K.; Nelson, S. M. *J. Am. Chem. Soc.* **1983**, *105*, 1924.
(29) König, E.; Ritter, G.; Kulshreshtha, S. K.; Goodwin, H. A. *Inorg. Chem.* **1983**, *22*, 2518.
(30) König, E.; Ritter, G.; Kulshreshtha, S. K.; Waigel, J.; Sacconi, L. *Inorg. Chem.* **1984**, *23*, 1241.
(31) Rao, C. N. R.; Rao, K. J. "Phase Transitions in Solids"; McGraw-Hill: New York, 1978.

probable reason why it has not been possible to fit the observed time dependence, viz. Figure 6, to rate law kinetics. The observation that, when the sample was ground, the crystalline substance assumed the behavior of a semisolid material indeed supports our assumption that rather loosely bound α-picoline molecules are present at room temperature.

An important factor that may be responsible for differences associated with the spin transition is the successive cracking of the crystallites, on the cycling of temperature, as a consequence of the crystallographic phase change. The cracking may produce the different shape of the hysteresis loop that has been observed for the crystalline substance (cf. Figures 2 and 3). Moreover, the cracking affects the relative intensity of X-ray diffraction peak profiles by changing the texture of the sample; thus it does not allow the estimation of the high-spin fraction from the area ratios.

Another observation of importance is the significant reduction in the width of the hysteresis loop and the almost continuous character that the spin transition assumes on grinding of the crystalline absorber. Simultaneously, the residual fraction of both the $^5T_2$ and $^1A_1$ phases increased considerably. In view of the above discussion, the number of defects will be increased on grinding of the material due to the surface effects and the migration of α-picoline molecules. This will result in a nonuniform environment for a large fraction of molecules and thus will give rise to a distribution of $T_c$ values. In addition, a certain number of crystallites will have a size below the critical size as a result of grinding and thus will not be able to participate in the crystallographic phase change and the associated spin transition. The observed reduction in the values of $\Delta T_c$ is thus arising due to a distribution of $T_c\uparrow$ and $T_c\downarrow$ values and an increase in the residual $^5T_2$ and $^1A_1$ fractions. The first-order nature of the transition is nonetheless maintained, evidence being the observed hysteresis. Similar results have been reported by Haddad et al.[32] for the grinding and doping effects in the iron(III) complex $[Fe(3\text{-}OCH_3SalEen)_2]PF_6$, where 3-$OCH_3$SalEen is the monoanion of ((ethylamino)ethyl)(3-methoxysalicylidene)amine and recently for $[Fe(phen)_2(NCS)_2]$.[23] For these complexes, the residual fractions are a sensitive function of the extent of grinding.

The difference of $\Delta E_Q$ values for both spin phases that was found for the different sets of observations is not easy to understand. For the $^5T_2$ phase, the difference is quite pronounced in the higher temperature region, where fitting uncertainties are small. For the $^1A_1$ phase, the difference is much smaller and is confined to the region above $T_c$. We believe that the encountered differences may be another consequence of the structural relaxations that are associated with the migration of α-picoline molecules in the lattice.

**Acknowledgment.** We appreciate financial support by the Stiftung Volkswagenwerk and the Fonds der Chemischen Industrie.

**Registry No.** $[Fe(4,7\text{-}(CH_3)_2phen)_2(NCS)_2]\cdot$α-pic, 43105-53-9.

(32) Haddad, M. S.; Federer, W. D.; Lynch, M. W.; Hendrickson, D. N. *Inorg. Chem.* **1981**, *20*, 131.

Contribution from the Departments of Chemistry, McMaster University, Hamilton, Ontario, Canada L8S 4M1, and University of California, Berkeley, California 94720

# Iodine-127 Mössbauer Study of Some Phenyl–Iodine Compounds and the Alkane-Activating Manganese Porphyrin Complexes Containing Iodosylbenzene Ligands

THOMAS BIRCHALL,*[1] JOHN A. SMEGAL,[2] and CRAIG L. HILL*[2,3]

*Received September 19, 1983*

Iodine-127 Mössbauer spectra at 4.2 K have been obtained on several compounds that contain the phenyl–iodine moiety including the alkane-activating Mn porphyrin complexes containing iodosylbenzene ligands, $[XMn^{IV}TPP(OIPh)_2]O$, X = Cl, Br (**1-Cl** and **1-Br**, respectively), that were recently purified and characterized. The relation of the $^{127}I$ Mössbauer parameters and the structural parameters of several iodine(III) compounds strongly implies that the observed positive quadrupole constants (2410–2507 MHz) and large asymmetry parameters (0.47–0.79) of these compounds reflect a disruption of the classical T-shape symmetry around I(III) by the proximity of a fourth ligand. The $^{127}I$ Mössbauer parameters for **1-Cl** and **1-Br** are similar to those of the other I(III) compounds, but quite distinct from those of I(I) or I(V) compounds. The iodine(III) in each of complexes **1** is coordinated by carbon, oxygen, and halogen atoms to give distorted T-shaped arrangements.

The interaction of iodosylbenzene with Mn(III) porphyrins in nonpolar, relatively inert organic media leads to the production of at least five types of isolable high-valent Mn porphyrin complexes depending on the axial ligand and the reaction conditions.[4–8] The most intriguing of these isolable species are the $[XMn^{IV}TPP(OIPh)]_2O$ (X = Cl or Br; TPP = tetraphenylporphinato dianion) complexes, **1**.[7] These complexes are not only unique with regard to their chemical properties but also highly unusual with regard to some of their physical and structural properties.[7] Complexes **1** are capable of replacing unactivated alkane C–H bonds with both C–O and C–X bonds (X = Cl or Br) at temperatures below 0 °C.[9]

(1) McMaster University.
(2) University of California, Berkeley.
(3) Correspondence to C.L.H. should be sent to Department of Chemistry, Emory University, Atlanta, GA 30322.
(4) Schardt, B. C.; Hollander, F. J.; Hill, C. L. *J. Am. Chem. Soc.* **1982**, *104*, 3964.
(5) Camenzind, M. J.; Hollander, F. J.; Hill, C. L. *Inorg. Chem.* **1982**, *21*, 4301.
(6) Hill, C. L.; Hollander, F. J. *J. Am. Chem. Soc.* **1982**, *104*, 7318.
(7) Smegal, J. A.; Schardt, B. C.; Hill, C. L. *J. Am. Chem. Soc.* **1983**, *105*, 3510.
(8) A second type of complex, $[AcO(PhIO)]_2Mn^{IV}TPP$, containing iodosylbenzene moieties as ligands to a transition metal was recently isolated, purified, and characterized: Smegal, J. A.; Hill, C. L. *J. Am. Chem. Soc.* **1983**, *105*, 2920.
(9) Smegal, J. A.; Hill, C. L. *J. Am. Chem. Soc.* **1983**, *105*, 3515.

0020-1669/84/1323-1910$01.50/0 